Development of human skin equivalents to unravel the impaired skin barrier in atopic dermatitis skin

Eweje, M.O.

CHAPTER 6

An *ex vivo* human skin model for studying skin barrier repair

Danso MO, Berkers T, Mieremet A, Hausil F, Bouwstra JA.
Exp Dermatol. 2015 Jan;24(1):48-54.

Abstract

In the studies described in this paper, we introduce a novel *ex-vivo* human skin barrier repair model. To develop this, we removed the upper layer of the skin, the stratum corneum (SC) by a reproducible cyanoacrylate stripping technique. After stripping the explants, they were cultured *in vitro* to allow the regeneration of the SC. We selected two culture temperatures 32°C and 37°C and a period of either 4 or 8 days.

After 8 days of culture, the explant generated SC at a similar thickness compared to native human SC. At 37°C, the early and late epidermal differentiation program was executed comparably to native human skin with the exception of the barrier protein involucrin. At 32°C, early differentiation was delayed, but the terminal differentiation proteins were expressed as in stripped explants cultured at 37°C. Regarding the barrier properties, the SC lateral lipid organization was mainly hexagonal in the regenerated SC, whereas the lipids in native human SC adopt a more dense orthorhombic organization. In addition, the ceramide levels were higher in the cultured explants at 32°C and 37°C than in native human SC. In conclusion, we selected the stripped *ex vivo* skin model cultured at 37°C as a candidate model to study skin barrier repair since epidermal and SC characteristics mimic more closely the native human skin than the *ex vivo* skin model cultured at 32°C. Potentially, this model can be used for testing formulations for skin barrier repair.

Introduction

The skin being the largest organ of the body (1.5m² in adults) provides protection for the body's interior against the external environment. This barrier function is mainly located in the outermost layer, the stratum corneum (SC) (1). The SC provides an excellent barrier against excessive water loss and penetration of pathogens and allergens through the skin (2, 3). The SC is 10-15µm thick with 15-20 corneocyte layers (4, 5) and its organization has been described as "brick-and-mortar" structure (6). The bricks represent the terminally differentiated corneocytes and the mortar the intercellular lipid matrix surrounding the corneocytes (7, 8). The SC lipid composition and organization plays an important role in the barrier function of the skin because the major pathway for penetration of molecules through the SC is via the SC lipid matrix (9-11). The main lipid classes in native human SC are free fatty acids (FFAs), ceramides (CERs) and cholesterol which form two lamellar phases. These include the short periodicity phase (SPP) and the long periodicity phase (LPP) with repeat distances of approximately 6nm and 13nm respectively (12). Within the lipid lamellae, the lipids are mainly organized in a dense orthorhombic packing, although a fraction of lipids adopt a hexagonal packing (13, 14). Within the epidermal strata, tight junction (TJ) proteins are known to contribute to the inside-outside barrier. They form an intercellular barrier between the epidermal cells and function to control the selective movement of water and ions through the epidermis (15) and regulate cell proliferation and differentiation (16, 17).

Atopic dermatitis (AD), dry skin conditions, 1st degree burns and sunburned skin are examples of skin conditions associated with impaired skin barrier function (18-20). In order to develop novel formulations or active components to enhance skin barrier repair, *in vitro* models are required. Currently, skin barrier repair is mainly studied in animals. This does not provide an optimal situation for translation into humans as the morphology in combination with SC properties of animal skin varies greatly from human skin (21-23). Furthermore, removal of SC from animals causes stress and animal testing of cosmetic products and ingredients have been banned in the European union since 2009. Consequently, the use of *in vitro* human skin barrier repair models can play an important role in screening formulations (24-27).
Currently, no appropriate *in vitro* human skin models are available to study skin barrier repair. The available human skin equivalents may offer a possibility however, applying formulations can only be performed during generation of the human skin equivalents. This is very labor intensive and needs dedicated expertise. In addition, an impaired barrier induced by tape stripping cannot be performed with human skin equivalents, due to the poor epidermal/dermal adhesion (28).In the present study, we introduce an *ex vivo* human skin model to study skin barrier repair. Using a reproducible cyanoacrylate stripping technique to remove SC from *ex vivo* human skin, we investigated the regrowth of SC *in vitro* by characterizing the epidermal morphogenesis, differentiation, SC lipid composition and organization. Potentially, this skin barrier repair model can be used for optimizing formulations and active ingredients to study their effect on skin barrier repair. The results show that the stripped skin cultured for 8 days at body temperature (37°C) or skin temperature (32°C) has an actively proliferating and differentiating epidermis resulting in the regeneration of SC *in vitro*. In addition, the regenerated SC lipids are organized in a crystalline lamellae with the presence of the same SC lipid classes and subclasses as seen in native human SC, with some interesting differences.

Materials and methods

Stripping of SC with cyanoacrylate

Human breast skin was obtained from Caucasian skin donors (aged 25-42 years) after written informed consent and handled according to Declaration of Helsinki principles. The skin was dermatomed at 400µm using a Padgett Electro Dermatome (Model B, Kansas city, KS, USA). 18mm punch biopsies of the dermatomed skin were used as a control. 26mm biopsies from the dermatomed skin were fixed into a custom made stripping device (see Supplementary figure S1). A single droplet of preheated cyanoacrylate (Pattex Gold original, Henkel, Dusseldorf, Germany) at 40°C was spread on a 20mm diameter stainless steel cylinder preheated to 40°C. The cylinder with cyanoacrylate was immediately placed on the skin. Standardized pressure was applied on the cylinder using a 2kg weight. After 2 minutes the cylinder was removed in one stroke and in alternating directions to ensure even removal of the SC from the skin surface. This stripping procedure was repeated until the skin gave a glossy appearance indicating that most of the SC has been removed (4-5 strips were required to remove the stratum corneum). The unstripped skin at the border of the biopsy was removed using a scalpel, yielding stripped biopsies of 18mm in diameter. From each donor, at least one stripped skin biopsy was used as control to analyze the number of corneocyte layers remaining on the stripped skin surface by safranin-O-red staining (described below). Stripped and non-stripped biopsies were cultured as described below.

Culture procedure

Non-stripped biopsies (served as controls) and stripped biopsies were washed thrice in sterile phosphate buffered saline (PBS, Braun, Melsungen, Germany) and placed in transwell filter inserts (Corning Life sciences, Amsterdam, Netherlands). The skin biopsies (referred to as explants) were cultured at air-liquid interface for 4 days or 8 days at 37°C or 32°C, 90% relative humidity and 7.3% CO2. The culture medium contained DMEM and Ham's F12 (Invitrogen, The Netherlands) (3:1 v/v) supplemented with 0.5µM hydrocortisone (Sigma), 1µM isoproterenol (Sigma), 10µM L-carnitine (Sigma), 10mM L-serine (Sigma), 0.053µM selenious acid (Johnson Matthey, Maastricht, The Netherlands), 0.5µg/mL insulin (Sigma), 1µM α-tocopherol acetate (Sigma), 1% penicillin/streptomycin, 25mM vitamin C (Sigma) and a lipid mixture of 7µM arachidonic acid (Sigma), 30 µM linoleic acid (Sigma) and 0.25µM palmitic acid (Sigma). The medium was refreshed twice a week.

Safranin-O-red staining

The cultured skin explants and the non-cultured (stripped and non-stripped) control biopsies were cryofixed in Tissue-Tek O.C.T.™ (Sakura Finetek Europe B.V., The Netherlands). The sections were stained with Safranin-O as described previously (29). Cryofixed skin of 5µm thickness were stained with 1% (w/v) Safranin-O solution (Sigma) for one minute and thereafter incubated in 2% (w/v) KOH solution for 30 minutes to swell the corneocytes. Five microscopic images (from three donors) per explant or biopsy were taken at 64x magnification.

Morphology and Immunohistochemistry

The skin explants and controls were embedded in paraffin, cut at 5µm thickness and stained with haematoxylin (2mg/ml) and eosin (4mg/ml) for morphological analysis. Immunohistochemical analysis of keratin 10, filaggrin, loricrin, involucrin, Ki67, caspase 3, keratin 6, ß-glucosylcerebrosidase, steroyl-CoA desaturase and acid-sphingomyelinase expression was also performed on 5µm paraffin sections. The primary and secondary antibodies are listed in Supplementary table S1. For further details see supplementary materials and methods.

Lipid extraction and analysis

SC was isolated from the skin explants using trypsin digestion as described by de Jager et al (30). Briefly, the explants were incubated overnight in 0.1% trypsin solution at 4°C followed by incubation at 37°C for 1 hour after which the SC could be peeled off. Lipid extracts from 2 explants per condition, were pooled for lipid analysis. The SC lipids were extracted by a modified Bligh and Dyer procedure (31, 32). Briefly, liquid-liquid extraction from native human SC and cultured stripped and non-stripped explants was performed using 3 different ratios of a chloroform/methanol/water mixture (1:2:0.5/1:1:0/2:1:0). The extracts from the three mixtures were pooled together after which 0.25M KCl solution was added to the pooled extract. The extract solution was washed with water and then the organic layer was collected after full separation of the water and organic layer. The collected organic layer was dried under a stream of nitrogen gas at 40°C and reconstituted in chloroform/methanol (2:1).

High performance thin layer chromatography (HPTLC): SC lipid composition was quantitatively analyzed by HPTLC (33) described in detail in the supplementary materials and methods.

Fourier transformed infra-red spectroscopy (FTIR) and Small angle x-ray diffraction (SAXD)

FTIR and SAXD measurements were performed as described earlier (34). The SC sheets were hydrated for 24 hours over a 27% NaBr solution prior to measurements. FTIR spectra were collected with a Varian 670-IR FTIR spectrometer (Agilent technologies, CA, USA), containing a broad-band mercury cadmium telluride detector, cooled with liquid nitrogen. SAXD patterns were detected with a Frelon 2000 CCD detector at room temperature for a period of 10 min using a microfocus as described by Bras et al., (35). 3 samples per condition were measured.

Statistical analysis

All statistical outcomes were determined using Graph-pad prism software and a two-tailed student's t-test to analyze the data.

Results

Stripped *ex vivo* skin generates SC *in vitro*

The skin was placed in a customized stripping device and using a customized metal cylinder coated with cyanoacrylate, the SC was removed sequentially (see Supplementary figure S1). The stripping procedure reduced the SC layers in the *ex vivo* skin explant from 13 ± 2 layers to 4 ± 2 layers (figure 1a,b) as determined by counting the number of corneocyte layers from five different spots of safranin-O stained sections. No difference was observed between the amount of SC removed in the central or boundary areas of the stripped skin. However, less SC at the furrows in the skin was removed compared to the flatter parts of the skin as described previously (36). After the removal of the SC, these biopsies were cultured to generate SC. After 4 days of culturing at 37°C, there was no significant increase in SC layers. However, after 8 days of culturing at 37°C, the SC layers of the stripped skin increased to 10 ± 3 layers (figure 1b). Decreasing the culture temperature to 32°C resulted in similar observations. After 4 days of culture no significant increase in the number of corneocyte layers was observed, but after extending to 8 days, the number of corneocyte layers increased to 10 ± 2 layers. Non-stripped controls were also cultured in the incubator for 4 and 8 days at 37°C and 32°C. After 8 days these non-stripped controls generated some additional corneocyte layers, but this increase was not as pronounced as with the stripped skin (figure 1b). Since our goal was to develop a skin barrier repair model, further analysis was performed using skin explants cultured for 8 days as the number of SC layers generated was closer to that in native human skin.

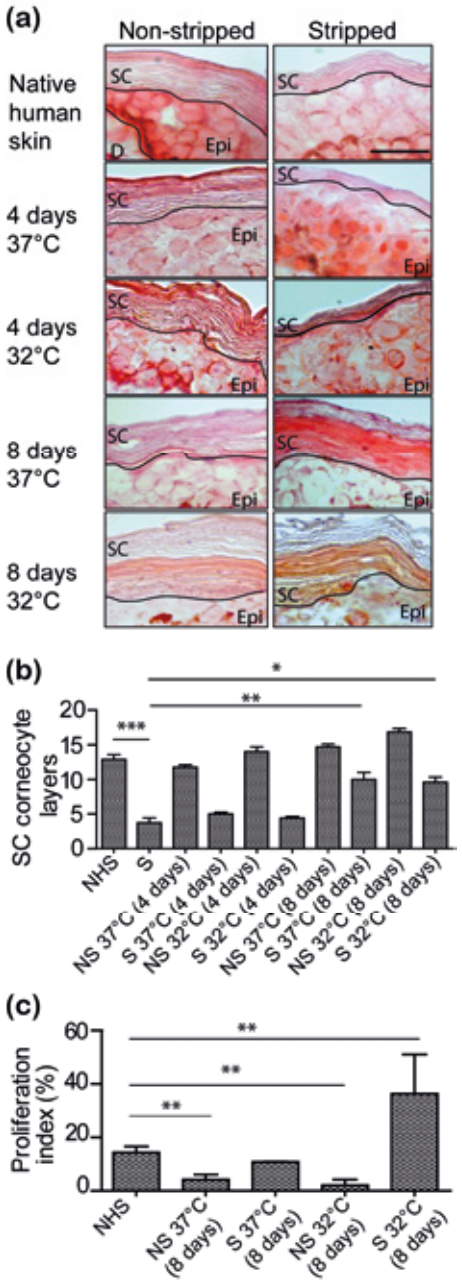

Figure 1: Stratum corneum (SC) layers and proliferation index in cultured *ex vivo* skin.(a) Swollen SC cell layers visualized by safranin-O staining. (b) The number of corneocyte layers was counted from safranin-O stained sections. The cyanoacrylate stripping procedure was efficient to remove the SC which was generated after 8 days of culturing at 37°C and 32°C. (c) Proliferation index of keratinocytes determined by Ki67 staining. The non-stripped skin explants cultured at 37°C and 32°C show decreased epidermal proliferation. At 37°C, the stripped explants show similar

proliferation as in native human skin and at 32°C, a 2x higher proliferation than native human skin. Data represent mean ± SEM of four donors. Five microscopic pictures were taken per explant analysis. Proliferation index was calculated from the number of Ki67 positive basal cells out of 100 counted basal cells from five microscopic images. Scale bar: 30µm, 64x magnification. NHS: native human skin, S:stripped, NS: non-stripped, Epi: viable epidermis, SC: stratum corneum, D:dermis *p<0.05, **p<0.01, ***p<0.001

Skin explants express epidermal differentiation proteins *in vitro*

Since SC is generated by cultured stripped skin explants, we examined their epidermal proliferation, morphology and epidermal differentiation. The proliferation index was calculated as the percentage of proliferating cells in the stratum basale by Ki67 staining. The proliferation index was drastically reduced in the non-stripped skin explants after 8 days of culture at 37°C and 32°C. In stripped explants cultured at 37°C, the proliferation was similar to native human skin while at 32°C proliferation was 2 fold higher compared to the native human skin (figure 1c). We also observe Ki67 positive cells in the first and second supra-basal layers of stripped explants cultured at 32°C. However, other conditions only showed basal cells positive for Ki67 (data not shown).

When focusing on the number of viable epidermal cell layers, the cultured explants showed similar number of viable cell layers as in native human skin with the exception of the stripped explants cultured at 32°C. These showed a significant increase in the number of viable epidermal cell layers from 6±1 layers in the native skin to 10±1 layers in the stripped skin ($p<0.01$, data not shown).

The stripped and non-stripped skin explants cultured at 37°C and 32°C show a normally differentiated epidermis. However in stripped explants cultured at 32°C, the terminal differentiation is not completely executed demonstrated by nuclei remnants in the SC (indicated by arrows, figure 2).

The early and terminal epidermal differentiation program was correctly executed in explants cultured at 37°C with the exception of involucrin and to a lesser extent filaggrin. Similar to control skin, keratin 10 (K10) was expressed in all suprabasal layers of the epidermis while loricrin and filaggrin were expressed in the stratum granulosum. However, the number of cell layers positive for filaggrin increased to 2-3 layers in both the stripped and non-stripped explants compared to 1 layer in control skin. Conversely, involucrin expression in the skin explants was observed in all epidermal layers in contrast to the stratum granulosum in native human skin.

When the culture temperature was reduced to 32°C, K10 expression was delayed in the stripped explants as 2-4 epidermal layers were negative for K10 expression (indicated by an arrow, figure 2). Loricrin and filaggrin were expressed as in native human skin in both stripped and non-stripped skin explants. However, the number of cell layers positive for filaggrin was also increased in both the stripped and non-stripped explants compared to control skin. In addition, involucrin was expressed in all epidermal layers in stripped and non-stripped explants cultured at 32°C (figure 2).

Analysis of keratin 6 (K6) expression in the explants showed that native human skin and non-stripped explants show little or no expression of K6 in the suprabasal layers of the epidermis. Conversely, stripped explants cultured at both temperatures showed a marked increase of K6 expression in the epidermis (supplementary figure S5). In addition, the expression of caspase 3 in the stripped and non-stripped explants cultured at 32°C and 37°C was very similar to native human skin: the expression of caspase 3 is present in the entire epidermis in all conditions (supplementary figure S5).

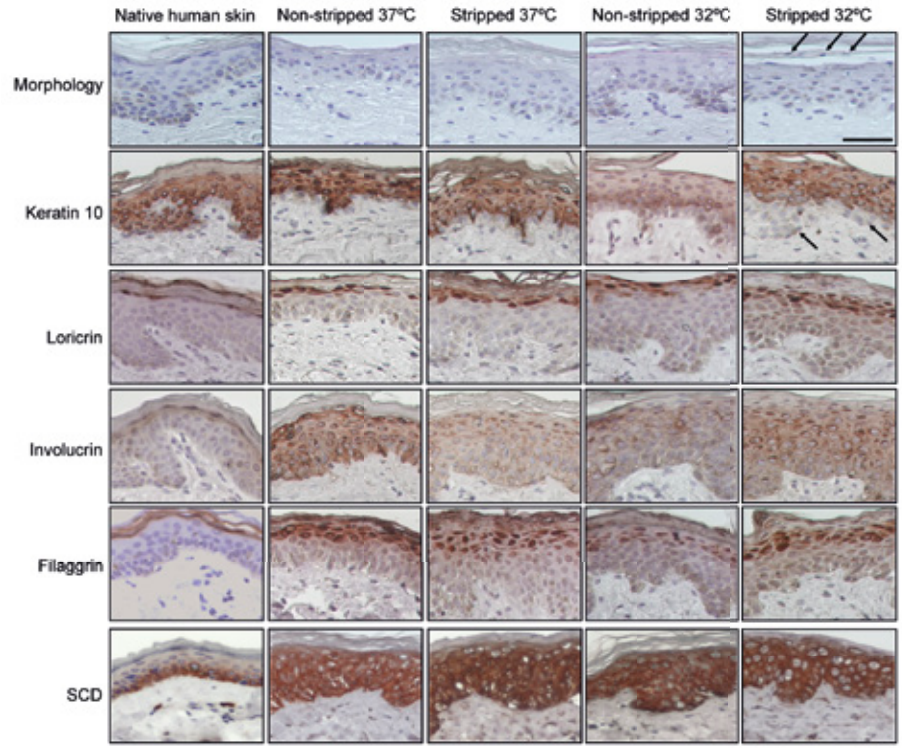

Figure 2: Morphology and epidermal differentiation in native human skin compared to non-stripped and stripped explants cultured for 8 days. Haematoxylin and eosin staining for morphological overview and immunohistochemical staining for keratin 10 (K10), Loricrin (LOR), involucrin (INV) and filaggrin (FLG). The stripped and non-stripped explants still display a differentiated epidermis at 37°C but at 32°C parakeratosis is observed mainly in the SC of the stripped explants (indicated by arrows). At 37°C, the non-stripped and the stripped explants express keratin 10, loricrin and filaggrin with similar localization as in the native human skin. The expression of involucrin in stripped and non-stripped explants was shifted to all epidermal layers rather than in the stratum granulosum. Non-stripped and the stripped explants cultured at 32°C also express filaggrin and loricrin as in native human skin however, the expression of keratin 10 is delayed and involucrin is expressed in all epidermal layers as with explants cultured at 37°C. Scale bar: 25µm. Images are representative of results consistently observed in three different skin donors. NHS: native human skin, S:stripped, NS: non-stripped

In vitro generated SC from stripped skin shows a similar lamellar lipid organization as native human SC but differences in the lateral packing

The SC lipid properties of the cultured explants were examined in relation to native human SC (the control). The lateral packing was examined using the CH_2 rocking vibrations of the lipid chains in the FTIR spectra from 0°C-90°C. A hexagonal lipid organization is portrayed by a single peak at 719cm^{-1} and an orthor-

hombic lipid packing by two vibrations at 719cm^{-1} and 730cm^{-1} in the spectrum. At 0°C, the lipids from native human SC adopt an orthorhombic lateral packing demonstrated by two strong contours at 719cm^{-1} and 730cm^{-1} (figure 3a). Around 42.5°C ± 2.5°C, the orthorhombic packing is converted into an hexagonal packing. This is characterized by a transition from a doublet to a singlet at 719cm^{-1}. The non-stripped skin explants cultured at 37°C show an orthorhombic lateral packing until 40.5°C ± 5.3°C (figure 3b). However, the stripped explants cultured at both temperatures show a strong peak at 719cm^{-1} and a small peak at 730cm^{-1} at 0°C (figure 3c,e). The orthorhombic packing is only present until 20.7°C ± 1.2°C and 29.3 ± 4.2°C at 37°C and 32°C, respectively i.e. the lipids are mainly organized in a hexagonal packing with a small population of lipids still forming an orthorhombic packing.

The conformational order of the lipids was also investigated using the thermotropic behaviour of the CH_2 symmetric stretching frequencies in the spectrum. In a crystalline organization (orthorhombic or hexagonal packing) the conformational order is high with CH_2 symmetric stretching frequencies <2850cm^{-1}. In a disordered organization (liquid phase), the CH_2 symmetric stretching frequencies are ≥ 2852cm^{-1}. Since the order-disorder transition occurs within a temperature range, the mid-point temperature at which the lipid domains change from an ordered state to a disordered liquid state was determined (37) i.e. "Mid-point Transition Temperature" (MTT). The results show that the MTT of the lipids in the regenerated SC of the stripped skin explants (37°C and 32°C) is significantly lower than in non-stripped cultured controls and native human SC ($p<0.05$, figure 3f). The CH_2 stretching frequency at skin temperature (32°C) was also increased in the stripped skin explants cultured at 37°C compared to the non-stripped explants ($p<0.05$, supplementary figure S2). This indicates an increased conformational disorder in the regrown SC of the stripped explants.

The lamellar lipid organization was also examined in the stripped and non-stripped explants in relation to native human skin using SAXD. In native human SC, the diffraction profiles show three diffraction peaks indicating the 1st, 2nd and 3rd order diffraction peak of the LPP (depicted by 1, 2 and 3,) and crystalline cholesterol domains, indicated by an asterisk (*). Peak "2" in native human skin represents both LPP (2nd order) and SPP (1st order). The stripped and non-stripped explants cultured at 37°C show a very similar profile, and exhibit a 1st - 3rd order diffraction peak of the LPP and crystalline cholesterol (supplementary figure S3). As the 1st order peak of the SPP is partly obscured by the 2nd order of the LPP, the presence of the SPP should induce a broadening of this peak. However, we could not obtain evidence for this broadening and thus the presence of this phase. In addition, the explants cultured at 32°C show similar diffraction profiles as in explants cultured at 37°C (data not shown).

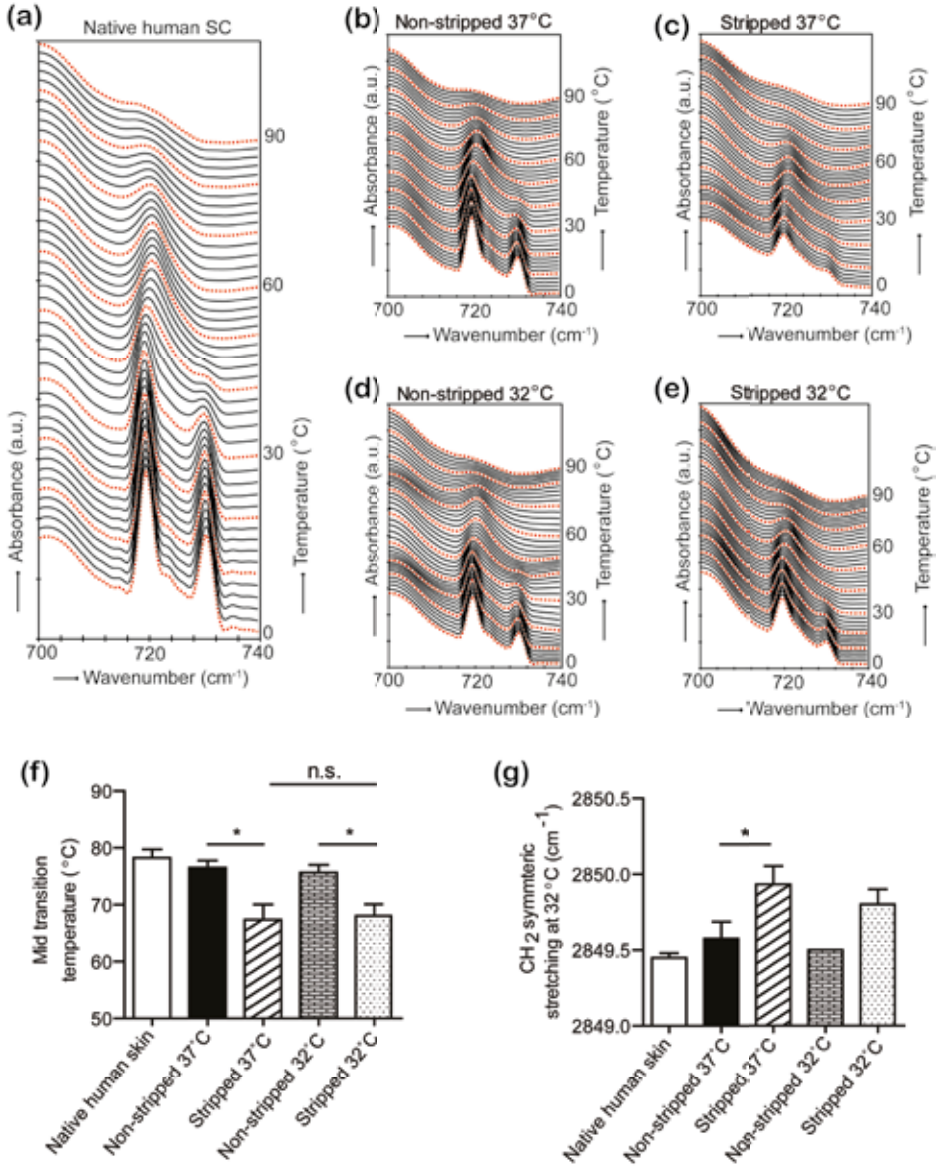

Figure 3: FTIR spectra showing the CH_2 rocking vibrations in the spectra of the stratum corneum (SC) of generated stripped explants as a function of temperature (0°C-90°C). (a) Native human SC and (b) non-stripped explants cultured at 37°C and (d) 32°C, show an orthorhombic lateral organization. The peak intensity of the 730cm^{-1} band is reduced in stripped explants cultured at (c) 37°C and (e) 32°C suggesting a higher population of lipids adopting a hexagonal organization. (f) Mid-point transition temperature (MTT). Data represents mean ± SEM from three donors, n.s.: not significant, *p<0.05, NHS: native human skin, S:stripped, NS: non-stripped

Generated SC from stripped explants contain the main SC lipid classes

The SC generated by the explants after stripping contains the main SC lipid classes CERs, FFAs and cholesterol with some changes in the distribution of these lipid classes as analyzed by HPTLC. The generated SC at 37°C and 32°C showed significantly higher CER levels respectively compared to native human skin (figure 4b, p=0.03 and p=0.06 respectively, for relative values see supplementary figure S4). In addition, the non-stripped controls cultured at both temperatures show a similar trend (figure 4b, p=0.04 and p=0.07, for relative values see supplementary figure S4).

All the CER subclasses detectable by HPTLC in native human skin were present in the generated SC cultured at both temperatures (figure 4c, for relative values see supplementary figure S2). However, some differences exist in the CER distribution of the cultured explants in relation to native human SC. At 37°C the levels of CER NS, EOH and AS/NH in regenerated SC were significantly increased compared to native human SC ($p<0.01$, $p<0.05$). Similarly, at 32°C the regrown SC showed significant increase in CER NS and AS/NH ($p<0.01$, $p<0.05$). The non-stripped explants cultured at 37°C and 32°C also have significantly more CER EOH and CER NS respectively than native human skin.

We further examined the expression of ß-glucosylcerebrosidase (GBA) and acid-sphingomyelinase (aSmase) involved in the synthesis of CERs from CER precursors. The expression of aSmase in the human epidermis shows a gradient from the basal layer to the granular layer with the highest expression seen in the granular layer. In all cultured explants, the expression of aSmase is similar in most epidermal layers (figure 4d). In native human epidermis, the expression of GBA is localized in the interface between the granular layer and SC. In explants cultured at 32°C or at 37°C, the localization of GBA expression is the same as native human epidermis.

Changes in unsaturated FFA levels have been shown to be involved in SC lipid organization. Therefore, we also examined the expression of steroyl CoA desaturase (SCD) which mono-unsaturates FFAs. SCD expression is seen in the basal layer of the epidermis in native human skin but in non-stripped and stripped explants cultured at 32°C and 37°C the expression of SCD is extended to all epidermal layers (figure 4d).

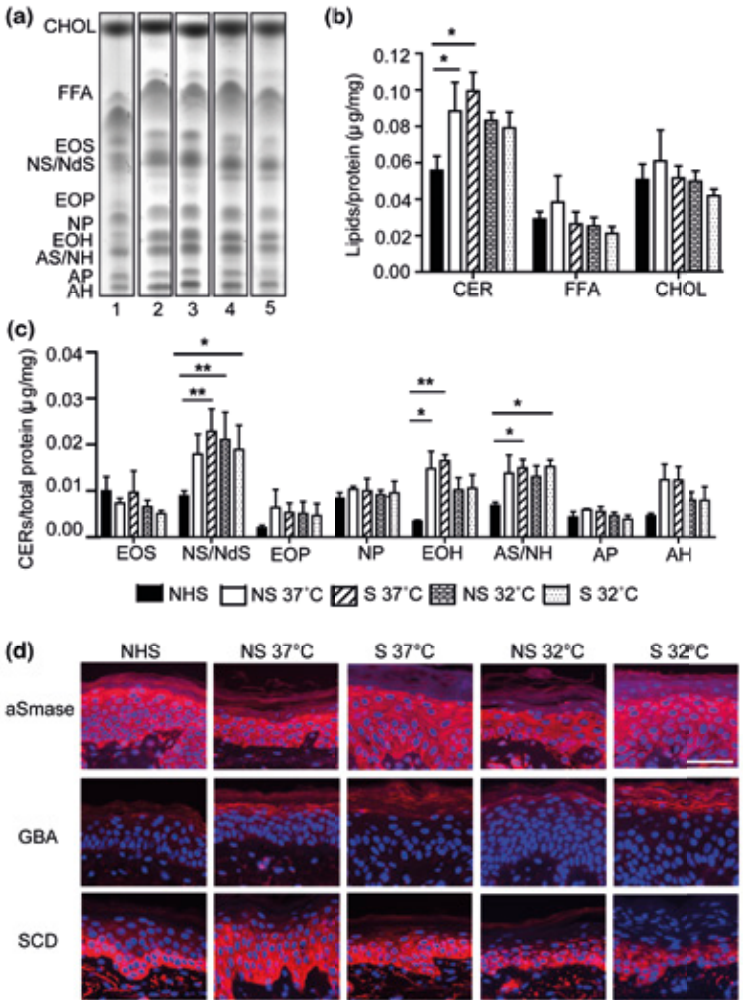

Figure 4: Stratum corneum (SC) lipid composition and epidermal expression of lipid synthesis enzymes in cultured *ex vivo* skin. (a) The lipids were separated according to the solvent system provided in supplementary table S2. 1-Native human skin, 2-Non-stripped 37°C, 3-Stripped 37°C, 4-Non-stripped 32°C, 5-Stripped 32°C (b) Absolute levels of cholesterol (CHOL), free fatty acids (FFA) and ceramides (CERs) (c) Absolute CER subclasses in cultured *ex vivo* skin. The SC from the non-stripped and stripped explants contains all CER subclasses in native human SC which are visible by high performance thin layer chromatography (HPTLC). (d) Immunohistochemical analysis of acid-sphingomyelinase (aSmase), ß-glucosylcerebrosidase (GBA) and steroyl CoA desaturase (SCD). Data represents mean ± SEM from three donors. Scale bar 25µm. NHS: native human skin, S:stripped, NS: non-stripped

Discussion

The aim of this study was to establish a human skin model to study skin barrier repair by i) removal of SC from *ex vivo* skin and ii) generation of the SC during *in vitro* culturing of stripped skin. We established a reproducible method of SC removal using a cyanoacrylate stripping technique which served as a starting point. After 8 days of culturing the stripped explants at 32°C and 37°C, the number of SC layers regrown was similar to the SC layers before stripping. The recovery of SC to control thickness after stripping *in vivo* ranges from 3-6 days in the arm and leg (38). In addition, barrier recovery (calculated by recovery of trans epidermal water loss values to baseline) after SC removal by tape-stripping in human facial skin reaches ~90% after 1 week and 100% recovery at 4 weeks (39). Duplan et al., presents an *ex vivo* human skin model for irritation/repair using SDS and vasointestinal peptide (40). In order to restore native epidermal features, the skin is treated with hydroxydecine in culture. Our present study examines skin barrier repair by removal of stratum corneum and culturing without the addition of a formulation and is thus a different approach.

Epidermal morphology and SC layers at the end of the 8 days culture period at both temperatures are similar to that of native human skin. However, the stripped explants cultured at skin temperature (32°C) exhibit parakeratotic epidermis, a feature also observed after repeated tape-stripping *in vivo* (41). This may occur from increased proliferation induced by stripping as nuclei are observed only in the lower layers of the SC. Parakeratosis is associated with a hyper proliferative epidermis, delayed K10 expression, increased involucrin expression and increased number of epidermal cell layers positive for filaggrin (41, 42). All of these characteristics are observed in stripped skin explants cultured at 32°C. Stripped explants cultured at 37°C also display increased filaggrin and involucrin expression, but very importantly no parakeratosis and no delayed expression of K10 is observed.

Proliferation (Ki67 expression) of stripped explants cultured at 37°C is similar to native human skin but at 32°C, proliferation is double that of native human skin. However, the number of SC layers generated after 8 days are similar at both temperatures. This may occur from the changes in proliferation index at 4 and 8 days of culture in the explants, as observed in a pilot study. At 4 days of culture, proliferation index in stripped explants cultured at 32°C is around 1% and 30% at 37°C (data not shown). However, after 8 days, the proliferation index is ~40% at 32°C and 12% at 37°C. This data suggests the increase in proliferation in stripped explants as a response to the SC removal is delayed at 32°C compared to 37°C. The number of corneocytes layers in the SC is an accumulative value and depends on the proliferation rate during the whole culturing period as no desquamation takes place.

The SC lipid properties in the stripped explants show several similarities to native human SC. The SC from the stripped and non-stripped explants cultured at 37°C contains the main SC lipid classes. However, we observe a significant increase in the absolute level of CERs in the explants cultured at 37°C and 32°C. Increase of CER levels also occurs in other full-thickness and epidermal human skin equivalents (43). Furthermore, when focusing on the CER subclasses, 10 different CER subclasses can be detected, of which CER NdS/NS and CER AS/NH cannot be separated. The composition of these CER subclasses is very similar to that in native human skin, although some important differences are also noticed. The increase in the level

of CERs was accompanied by a stronger staining for aSmase suggesting its role in the increased CER levels. ASmase catalyzes the conversion of sphingomyelin to ceramides. Sphingomyelin is a precursor of CER NS and AS (44, 45) and both are increased by approximately 2-3 fold in the cultured explants compared to native human SC. The change in environmental conditions and barrier disruption induces stress in keratinocytes. This may result in increased CERs via sphingomyelinases and up-regulation of the activity of serine palmitoyl-transferase and/or ceramide synthases in de novo CER synthesis (46, 47).

Disruption of the SC also results in the loss of the epidermal calcium gradient which is crucial for differentiation (48, 49). The loss of calcium gradient affects the expression of epidermal differentiation proteins including filaggrin and involucrin and may also contribute to the changes in involucrin and filaggrin expression in the cultured skin explants (50, 51). In non-stripped skin, we still observe increased CER levels and altered involucrin expression although there is no barrier disruption. The exact mechanism responsible for these changes in non-stripped explants remains unknown.

SC lipids generated by the stripped explants adopt mainly a hexagonal organization as opposed to an abundant orthorhombic organization in native human SC. The hexagonal lateral organization is also observed in epidermal or full thickness human skin equivalents (52). In these models an increased relative level of MUFAs was detected, which may be responsible for the abundant hexagonal packing (43, 52). Using lipid model systems we observed indeed that increased levels of MUFA enhances the formation of the hexagonal lateral packing (53). Therefore the hexagonal lipid organization in the generated SC in the explants may be attributed to an increased level of MUFAs resulting from increased SCD expression. The effect of increased SCD expression on lateral lipid organization is not observed in the non-stripped skin due to the very low amount of SC layers generated *in vitro* (1-2 layers) compared to the SC layers on the skin before culturing (13 ± 2 layers).

Some features of the cultured stripped skin can be observed in barrier related skin diseases such as increase in involucrin expression, CER NS, AS and hexagonal lipid organization (54-57). However, there are also aspects that do not resemble diseased skin e.g. increased CER EOS, similar levels of CER NP and filaggrin, loricrin expression as in native skin etc. This suggests that the cultured stripped skin generates some aspects of diseased skin, but is not a perfect model for diseased skin. The cultured stripped model also generates some important features especially seen in human skin equivalents and this might be induced by the culture conditions (48).

We suggest that culture of cyanoacrylate stripped skin explants provides a potential model to study i) skin barrier repair *ex vivo* and ii) investigating the effect of culture medium composition and environmental conditions during culture on the restoration of the skin barrier. Firstly, the SC lipid properties in regrown SC bear some aspects observed with altered skin barrier function (57-59) including reduced orthorhombic lipid organization and increased lipid conformational disorder of SC lipids. The presence of these characteristics in the cultured stripped explants can provide a system where formulations can be tested to enhance skin barrier repair.

Secondly, in the development of 3D *in vitro* skin models, no human skin equivalent fully mimics the SC lipid properties of native human skin (52, 60, 61). Our model shows some advantages over the available human skin equivalents when applied to optimization of culture conditions to mimic native human SC properties *in vitro*. This is because the culture period is shorter (14-21 days for human skin equivalents) and does not require cell isolation and seeding which saves time and is less labor intensive. It is also possible to examine inter-donor changes in these cultures with human skin.

In conclusion, the removal of SC from *ex vivo* skin and culture for 8 days at 37°C generates an *ex vivo* human skin model which possesses various similarities in epidermal properties to native human skin than at 32°C. Therefore this model has the potential to be used in studying skin barrier repair.

Acknowledgements

The authors thank the personnel at DUBBLE beam line (BM26), ESRF for assisting with X-ray measurements. This research was financially supported by Dutch Technology Foundation STW (grant no. 12400).

References

1. Burton R F. Estimating body surface area from mass and height: Theory and the formula of Du Bois and Du Bois. Ann Hum Biol 2008: 35: 170-184.
2. Proksch E, Brandner J M, Jensen J-M. The skin: an indispensable barrier. Exp Dermatol 2008: 17: 1063-1072.
3. Madison K C. Barrier Function of the Skin: "La Raison d'Etre" of the Epidermis. J Investig Dermatol 2003: 121: 231-241.
4. Holbrook K A, Odland G F. Regional differences in the thickness (cell layers) of the human stratum corneum: an ultrastructural analysis J Investig Dermatol 1974: 62: 415-422.
5. Blair C. Morphology and thickness of the human stratum corneum Br J Dermatol 1968: 80: 430-436.
6. Michaels A S, Chandrasekaran S K, Shaw J E. Drug permeation through human skin: Theory and invitro experimental measurement. AIChE Journal 1975: 21: 985-996.
7. Elias P M. Epidermal Lipids, Barrier Function, and Desquamation. J Invest Dermatol 1983: 80: 44s-49s.
8. Elias P. Epidermal lipids, membranes, and keratinization. Int J Dermatol 1981: 20: 1-19.
9. Bouwstra J A, Ponec M. The skin barrier in healthy and diseased state. Biochim Biophys Acta - Biomembranes 2006: 1758: 2080-2095.
10. ML. W, PM. E. The extracellular matrix of stratum corneum: role of lipids in normal and pathological function. Crit Rev Ther Drug Carrier Syst 1987: 3: 95-122.
11. Johnson M E, Blankschtein D, Langer R. Evaluation of solute permeation through the stratum corneum: Lateral bilayer diffusion as the primary transport mechanism. J Pharm Sci 1997: 86: 1162-1172.
12. Bouwstra J, Gooris G S, Spek v d, et al. Structural investigations of human stratum corneum by small-angle X-ray scattering. J Invest Dermatol 1991: 97: 1005-1012.
13. Bouwstra J, Pilgram G, Gooris G, et al. New Aspects of the Skin Barrier Organization. Skin Pharmacol Physiol 2001: 14(suppl 1): 52-62.
14. Damien F, Boncheva M. The Extent of Orthorhombic Lipid Phases in the Stratum Corneum Determines the Barrier Efficiency of Human Skin *In Vivo*. J Invest Dermatol 2009: 130: 611-614.
15. Anderson J M, Van Itallie C M. Physiology and Function of the Tight Junction. Cold Spring Harbor Perspectives in Biology 2009: 1.
16. Aijaz S, Balda M S, Matter K. Tight junctions: molecular architecture and function. Int Rev Cytol 2006: 248: 261-298.
17. Schneeberger E E, Lynch R D. The tight junction: a multifunctional complex. Am J Physiol Cell Physiol 2004: 286: C1213-1228.
18. Tupker R A, Pinnagoda J, Coenraads P J, et al. Susceptibility to irritants: role of barrier function, skin dryness and history of atopic dermatitis. Br J Dermatol 1990: 123: 199-205.
19. Elias P M, Hatano Y, Williams M L. Basis for the barrier abnormality in atopic dermatitis: Outside-inside-outside pathogenic mechanisms. J Allergy Clin Immunol 2008: 121: 1337-1343.

20. Church D, Elsayed S, Reid O, et al. Burn Wound Infections. Clin Microbiol Rev 2006: 19: 403-434.
21. Elias. P M, Feingold. K R, eds. Skin barrier. New York: Taylor & francis Group: 2006.
22. Caussin J, Gooris G S, Janssens M, et al. Lipid organization in human and porcine stratum corneum differs widely, while lipid mixtures with porcine ceramides model human stratum corneum lipid organization very closely. Biochimica et Biophysica Acta (BBA) - Biomembranes 2008: 1778: 1472-1482.
23. Mojumdar E H, Kariman Z, van Kerckhove L, et al. The role of ceramide chain length distribution on the barrier properties of the skin lipid membranes. Biochimica et Biophysica Acta (BBA) - Biomembranes 2014: 1838: 2473-2483.
24. Ehrlich H P. Understanding experimental biology of skin equivalent: from laboratory to clinical use in patients with burns and chronic wounds. The American Journal of Surgery 2004: 187: S29-S33.
25. Bello Y, Falabella A, Eaglstein W. Tissue-Engineered Skin. Am J Clin Dermatol 2001: 2: 305-313.
26. Garlick J. Engineering Skin to Study Human Disease - Tissue Models for Cancer Biology and Wound Repair. In: Lee K, Kaplan D, eds. Tissue Engineering II: Springer Berlin Heidelberg, 2007: 207-239.
27. Supp D M, Boyce S T. Engineered skin substitutes: practices and potentials. Clinics in Dermatology 2005: 23: 403-412.
28. Groeber F, Holeiter M, Hampel M, et al. Skin tissue engineering — *In vivo* and *in vitro* applications. Adv Drug Delivery Rev 2011: 63: 352-366.
29. Oudshoorn M H M, Rissmann R, Van Der Coelen D, et al. Development of a murine model to evaluate the effect of vernix caseosa on skin barrier recovery. Experimental Dermatology 2009: 18: 178-184.
30. de Jager M, Groenink W, Bielsa i Guivernau R, et al. A Novel *in vitro* Percutaneous Penetration Model: Evaluation of Barrier Properties with & P-Aminobenzoic Acid and Two of Its Derivatives. Pharmaceutical Research 2006: 23: 951-960.
31. Bligh E G, Dyer W J. A rapid method of total lipid extraction and purification. Can J Biochem Physiol 1959: 37: 911-917.
32. Thakoersing V S, Ponec M, Bouwstra J A. Generation of human skin equivalents under submerged conditions-mimicking the in utero environment. Tissue engineering Part A 2009: 16: 1433-1441.
33. Ponec M, Weerheim A, Lankhorst P, et al. New acylceramide in native and reconstructed epidermis. The Journal of investigative dermatology 2003: 120: 581-588.
34. Thakoersing V, Gooris G, Mulder A, et al. Unraveling barrier properties of three different in-house human skin equivalents. Tissue Eng Part C: Methods 2012 18: 1-11.
35. Bras W, Dolbnya I P, Detollenaere D, et al. Recent experiments on a small-angle/wide-angle X-ray scattering beam line at the ESRF. Journal of Applied Crystallography 2003: 36: 791-794.
36. van der Molen R G, Spies F, van 't Noordende J M, et al. Tape stripping of human stratum corneum yields cell layers that originate from various depths because of furrows in the skin. Arch Dermatol Res 1997: 289: 514-518.
37. Thakoersing V S, Danso M O, Mulder A, et al. Nature versus nurture: does human skin maintain its stratum corneum lipid properties *in vitro*? Experimental Dermatology 2012: 21: 865-870.
38. Bargo P R, Walston S T, Chu M, et al. Non-invasive assessment of tryptophan fluorescence and

confocal microscopy provide information on skin barrier repair dynamics beyond TEWL. Exp Dermatol 2013: 22: 18-23.
39. Gorcea M, Hadgraft J, Lane M E, et al. *In vivo* barrier challenge and long-term recovery in human facial skin. Int J Cosmet Sci 2013: 35: 250-256.
40. Duplan H, Questel E, Hernandez-Pigeon H, et al. Effects of Hydroxydecine(®) (10-hydroxy-2-decenoic acid) on skin barrier structure and function *in vitro* and clinical efficacy in the treatment of UV-induced xerosis. Eur J Dermatol **2011**: 21: 906-915.
41. Gerritsen M J P, Erp P E J, Vlijmen-Willems I M J J, et al. Repeated tape stripping of normal skin: a histological assessment and comparison with events seen in psoriasis. Arch Dermatol Res 1994: 286: 455-461.
42. Harrison C A, Layton C M, Hau Z, et al. Transglutaminase inhibitors induce hyperproliferation and parakeratosis in tissue-engineered skin. Br J Dermatol 2007: 156: 247-257.
43. Thakoersing V S, van Smeden J, Mulder A A, et al. Increased Presence of Monounsaturated Fatty Acids in the Stratum Corneum of Human Skin Equivalents. J Invest Dermatol 2013: 133: 59-67.
44. Gatt S. Enzymic Hydrolysis and Synthesis of Ceramides. J Biol Chem 1963: 238: PC3131-PC3133.
45. Uchida Y, Hara M, Nishio H, et al. Epidermal sphingomyelins are precursors for selected stratum corneum ceramides. J Lipid Res 2000: 41: 2071-2082.
46. Nikolova-Karakashian M N, Rozenova K A. Ceramide in Stress Response. In: Chalfant C, Poeta M, eds. Sphingolipids as Signaling and Regulatory Molecules: Springer New York, 2010: 86-108.
47. Uchida Y. Ceramide signaling in mammalian epidermis. Biochim Biophys Acta (BBA) - Molecular and Cell Biology of Lipids 2014: 1841: 453-462.
48. Menon G K, Elias P M, Feingold K R. Integrity of the permeability barrier is crucial for maintenance of the epidermal calcium gradient. Br J Dermatol 1994: 130: 139-147.
49. Menon G K, Elias P M, Lee S H, et al. Localization of calcium in murine epidermis following disruption and repair of the permeability barrier. Cell Tissue Res 1992: 270: 503-512.
50. Vicanová J, Boelsma E, Mommaas A, et al. Normalization of epidermal calcium distribution profile in reconstructed human epidermis is related to improvement of terminal differentiation and stratum corneum barrier formation. J Invest Dermatol 1998: 111: 97-106.
51. Torma H, Lindberg M, Berne B. Skin Barrier Disruption by Sodium Lauryl Sulfate-Exposure Alters the Expressions of Involucrin, Transglutaminase 1, Profilaggrin, and Kallikreins during the Repair Phase in Human Skin *In Vivo*. J Invest Dermatol 2007: 128: 1212-1219.
52. Varsha S. Thakoersing G S G, Aat Mulder, Marion Rietveld, Abdoelwaheb El Ghalbzouri, and Joke A. Bouwstra. Unraveling Barrier Properties of Three Different In-House Human Skin Equivalents. Tissue Engineering Part C: Methods 2012: 18: 1-11.
53. Mojumdar E H, Helder R W J, Gooris G, et al. Monounsaturated fatty acids reduce the barrier of stratum corneum lipid membranes by enhancing the formation of a hexagonal lateral packing. Langmuir 2014: 30: 6534-6543.
54. Chen J-Q, Man X-Y, Li W, et al. Regulation of Involucrin in Psoriatic Epidermal Keratinocytes: The Roles of ERK1/2 and GSK-3ß. Cell Biochem Biophys 2013: 66: 523-528.
55. Jensen J-M, Folster-Holst R, Baranowsky A, et al. Impaired Sphingomyelinase Activity and

Epidermal Differentiation in Atopic Dermatitis. J Investig Dermatol 2004: 122: 1423-1431.
56. Imokawa G, Abe A, Jin K, et al. Decreased Level of Ceramides in Stratum Corneum of Atopic Dermatitis: An Etiologic Factor in Atopic Dry Skin? J Investig Dermatol 1991: 96: 523-526.
57. van Smeden J, Janssens M, Gooris G S, et al. The important role of stratum corneum lipids for the cutaneous barrier function. Biochim Biophys Acta 2014: 1841: 295-313.
58. Janssens M, van Smeden J, Gooris G S, et al. Increase in short-chain ceramides correlates with an altered lipid organization and decreased barrier function in atopic eczema patients. J Lipid Res 2012: 53: 2755-2766.
59. Janssens M, van Smeden J, Gooris G S, et al. Lamellar Lipid Organization and Ceramide Composition in the Stratum Corneum of Patients with Atopic Eczema. J Invest Dermatol 2011: 131: 2136-2138.
60. Tfayli A, Bonnier F, Farhane Z, et al. Comparison of structure and organization of cutaneous lipids in a reconstructed skin model and human skin: spectroscopic imaging and chromatographic profiling. Exp Dermatol 2014: 23: 441-443.
61. Ponec M, Boelsma E, Gibbs S, et al. Characterization of Reconstructed Skin Models. Skin Pharmacol Physiol 2002: 15(suppl 1): 4-17.

Supplementary figures

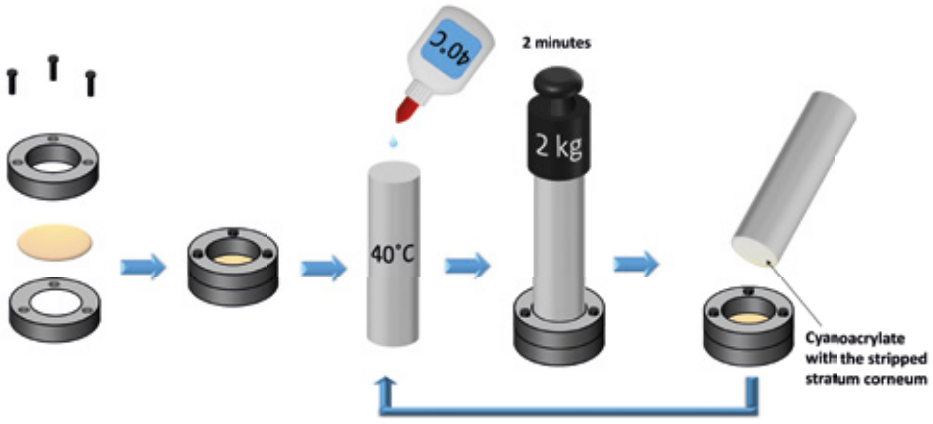

Supplementary figure S1: Stripping of stratum corneum (SC) from *ex vivo* skin. 26 mm skin biopsies of 400 µm thickness is fixed into a custom made cyanoacrylate stripping device. A single droplet of preheated cyanoacrylate (40°C) was spread on a 20 mm diameter stainless steel cylinder which was also preheated to 40°C. The cylinder with cyanoacrylate was immediately placed on the skin together with a 2 kg weight to achieve a standardized pressure for 2 minutes. The cylinder was removed in one move, with alternating directions of 180° to ensure even removal of the SC on both sides. This stripping procedure was repeated until the skin gave a glossy appearance indicating that most of the SC has been removed.

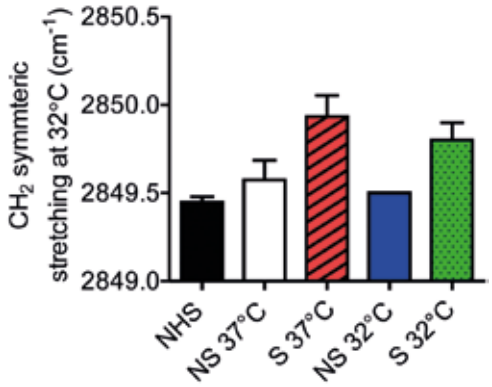

Supplementary figure S2: FTIR spectra showing the CH_2 symmetric stretching frequency at 32°C in the spectra of the stratum corneum (SC) of cultured explants. Data represents mean ± SEM from three donors, *p<0.05. NHS: native human skin, S:stripped, NS: non-stripped

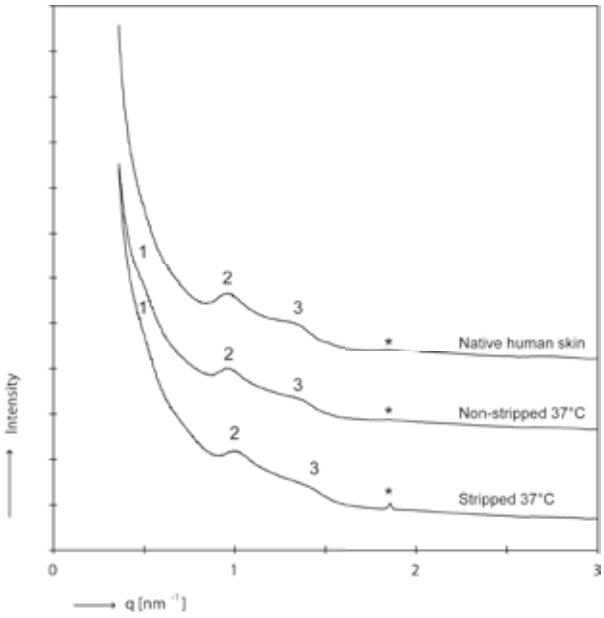

Supplementary figure S3: Representative x-ray diffraction pattern of SC from stripped, non-stripped explants and native human skin. 1, 2 and 3 indicate the 1st, 2nd and 3rd order of the long periodicity phase (LPP) respectively. The "2" peak from native human SC and non-stripped SC represent both the 2nd order of the LPP and the 1st order of the short periodicity phase (SPP) Therefore, the repeat distances cannot be calculated directly from this diffraction profile. Crystalline cholesterol is indicated by (*).

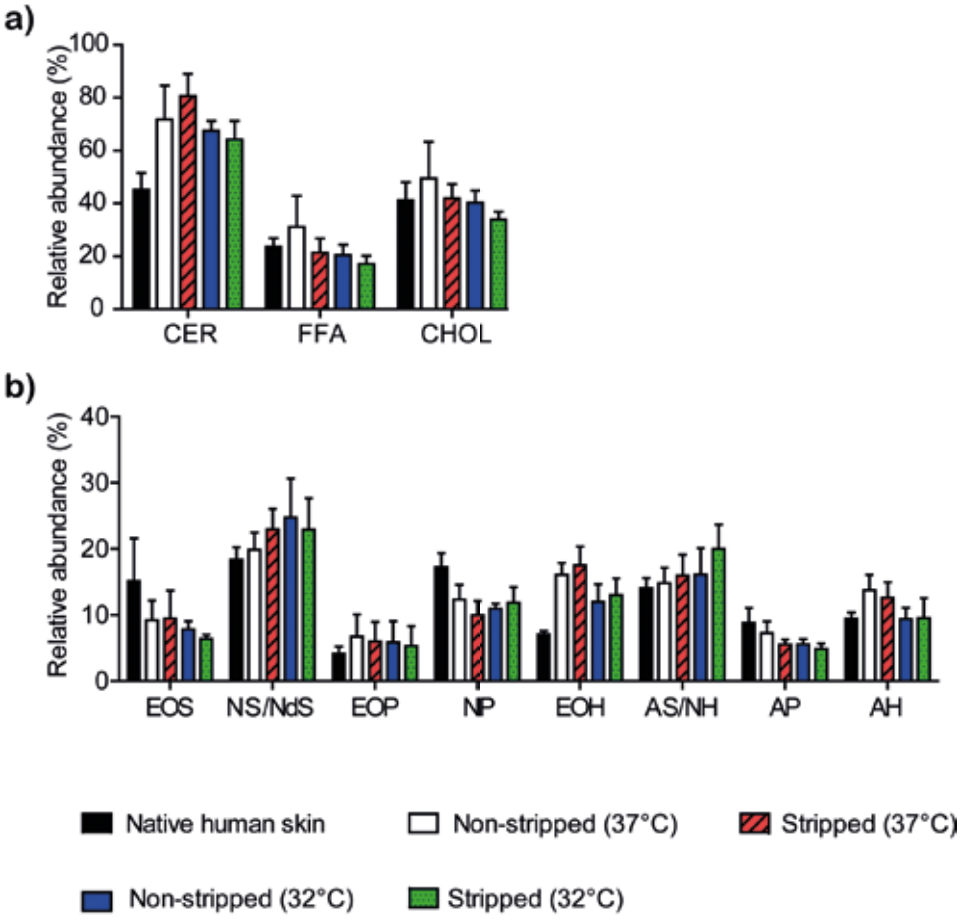

Supplementary figure S4: Relative levels of SC lipids in cultured explants. (a) Cholesterol (CHOL), free fatty acids (FFA) and ceramides (CERs) (b) various classes of CERs. Data represents mean ± SEM from three donors.

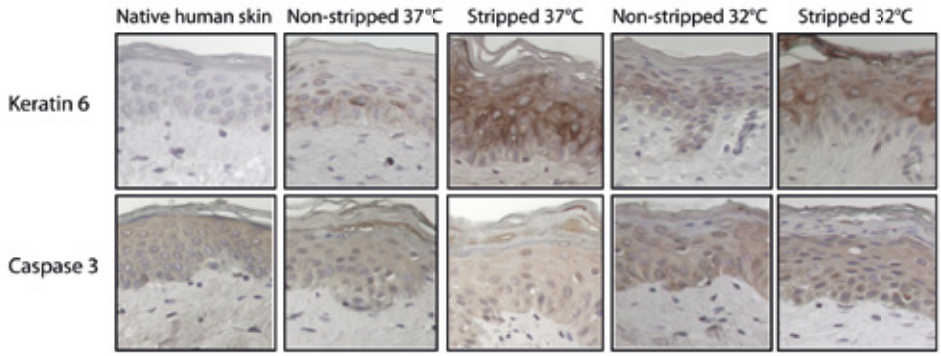

Supplementary figure S5: Immunohistochemical staining for keratin 6 and caspase 3. Images were taken at 20x magnification. Scale bar: 25µm

Supplementary tables

Table S1: Primary and secondary antibodies for immunohistochemical staining

Antibodies	Clone	Dilution	Company
Primary antibodies			
Mouse cytokeratin 10 Ab-2	DE-K10	1:800	Neomarkers, USA
Mouse filaggrin Ab-1	FLG01	1:800	Neomarkers, USA
Rabbit Loricrin	AF62	1:1200	Covance, USA
Mouse involucrin	SY5	1:1200	Sanbio, The Netherlands
Rabbit SCD	Polyclonal	1:100	Sigma-Aldrich
Rabbit Ki67	SP6	1:800	Neomarkers, USA
Rabbit acid-sphingomyelinase	Polyclonal	1:1000	Abcam, UK
Mouse β-glucosylcerebrosidase	IgG2a	1:400	Abcam, UK
Mouse α human keratin 6	LHK6B	1:5	Neomarkers
Rabbit Caspase 3	Polyclonal	1:50	BD Biosciences
Secondary antibody			
Biotinylated universal antibody, anti-rabbit/mouse IgG			Vector laboratories Burlingame, CA, USA
Rhodamine Red-X (Goat anti-rabbit) (IF)		1:300	Jackson immunoresearch Laboratory, USA
Cy3 (Goat Anti-Mouse) (IF)		1:1000	Jackson immunoresearch Laboratory, USA

Table S2: Solvent system used for barrier lipids analysis by thin layer chromatography

Eluent	Composition (v/v)	Distance (mm)
1	Dichloromethane/Ethylacetate/Acetone/Methanol (88:8:4:1)	40
2	Chloroform/Acetone/Methanol (76:8:16)	10
3	Hexane/Chloroform/Acetone/Methanol (6:80:12:2)	70
4	Hexane/Chloroform/Hexyl acetate/Acetone/ Methanol (6:80:0.1:10:4)	95

Table S3: Ceramide nomenclature

	Non hydroxy fatty acid (N)	α- hydroxy fatty acid (A)	Esterified ω-hydroxy fatty acid (EO)
Dihydrosphingosine (dS)	NdS	AdS	EOdS
Sphingosine (S)	NS	AS	EOS
Phytosphingosine (P)	NP	AP	EOP
6-hydroxy sphingosine (H)	NH	AH	EOH

The human stratum cornuem(SC) contains 4 sphingoid bases (dihydrosphingosine (dS), Sphingosine (S), phytosphingosine (P) and 6-hydroxy sphingosine (H)) and three acyl chains (non-hydroxy fatty acid (N), α-hydroxy fatty acid (A) and esterified hydroxy fatty acid (EO)). Together, these result in the 12 ceramide subclasses present in human SC.

Supplementary materials and methods

Morphology and Immunohistochemistry

The skin sections (except the sections stained for aSmase) were incubated in sodium citrate buffer (pH 6) for 30 minutes at 95°C for antigen retrieval. The sections stained for aSmase were incubated in sodium citrate buffer (pH 6) for 5 minutes at 110°C in an autoclave (Laboratory autoclave, model A275, Zirbus technology, Germany) for antigen retrieval. Thereafter, all sections were blocked with 2.5% normal horse serum (Vector laboratories Burlingame, CA) for 20 minutes and incubated overnight at 4°C with the primary antibody diluted in 1% bovine serum albumin (BSA) in PBS.

Staining procedure with amino-ethylcarbazole: Subsequently, the sections were incubated for 30 minutes at room temperature with the secondary antibody (Vector laboratories Burlingame, CA) and the ABC reagent (Vector laboratories Burlingame, CA) for 30 minutes and 10 minutes for caspase 3. The sections were washed with 0.1M sodium acetate buffer and incubated in amino-ethylcarbazole (Sigma) dissolved in N,N-dimethylformamide (1g/250mL) (Sigma) with 0.1% hydrogen peroxide for 30 minutes at room temperature. All sections were counterstained with haematoxylin.

Staining procedure for immunofluorescence: Sections were incubated with the appropriate secondary antibody for 1 hour at room temperature and mounted using DAPI Vectashield (Vector laboratories Burlingame, CA).

Proliferation index: Five microscopic images per explant or biopsy (from three donors) were taken at 20x magnification. For each image, the number of basal cells were counted and the proliferation index was calculated as the percentage of Ki67 positive cells within the basal layer of the epidermis.

High performance thin layer chromatography (HPTLC)

To identify the different classes of lipids, co-chromatography of a standard lipid mixture was performed. This included six subclasses of synthetic CERs (EOS, NS, EOP, NP, AS and AP (Evonik, Germany)), FFAs (stearic acid, tricosanoic acid, palmitic acid, behenic acid, arachidonic acid, cerotic acid and lignoceric acid (Sigma)) and cholesterol (Sigma). The ceramide nomenclature is according to the terminology of Motta et al., (1) and Masukawa et al., (2) which is used throughout this article (Supplementary table S3).

Lipid quantification by HPTLC: The standard lipid mixture and extracted lipids were sprayed on a silica gel plate (Merck, Germany) using a Camag Linomat IV device, (Muttenz, Switzerland) within a concentration range of 4µg-30µg. Variation in the amounts of sprayed standard lipids allowed the calculation of calibration curves for lipid quantification. The lipids were separated using organic solvent mixtures at specific running distances (supplementary table S2). The plate was stained with a copper acetate-copper sulfate solution (3:1) and charred at 170°C for 15 minutes. The images were obtained with a GS800 calibrated densitometer (Bio-Rad,CA, USA) and analyzed with quantity-one software 4.6.5 (Bio-Rad, CA, USA). The amount of each lipid class was determined from a non-linear fit of the calibration curve from its synthetic

lipid counterpart. This provided the relative levels of the various lipid classes. The absolute values were provided by weighing the SC before and after extraction.

Fourier transformed infra-red spectroscopy (FTIR) and Small angle x-ray diffraction (SAXD)

The SC sheets were hydrated for 24 hours over a 27% NaBr solution and sandwiched between AgBr windows (Pier-optics, Japan). The spectra were collected using a Varian 670-IR FTIR spectrometer (Agilent technologies, CA, USA), equipped with a broad-band mercury cadmium telluride detector, cooled with liquid nitrogen. The spectra were collected in transmission mode, as a co-addition of 256 scans at $1cm^{-1}$ resolution during 4 minutes from 0°C-90°C at a frequency range of $600\text{-}4000cm^{-1}$. The spectra was deconvoluted using enhancement factor of 1.7 and half-width of 5 cm^{-1} and analysed using Bio-Rad Win-IR Pro 3.0 software from Biorad (Biorad laboratories, MA, USA).

The samples were hydrated as described above and SAXD patterns were detected with a Frelon 2000 CCD detector at room temperature for a period of 10 min using a microfocus as described by Bras et al., (3). From the scattering angle, vector q was calculated from the following equation $q= (4\pi\sin\theta)/\lambda$. θ is the scattering angle and λ is the wavelength of the x-ray.

References

1. Motta S, Monti M, Sesana S, Caputo R, Carelli S, Ghidoni R. Ceramide composition of the psoriatic scale. Biochim Biophys Acta-Molecular basis of disease 1993: 1182: 147-151.
2. Masukawa Y, Narita H, Shimizu E, et al. Characterization of overall ceramide species in human stratum corneum. J Lipid Res 2008: 49: 1466-1476.
3. Bras W, Dolbnya I P, Detollenaere D, et al. Recent experiments on a small-angle/wide-angle X-ray scattering beam line at the ESRF. Journal of Applied Crystallography 2003: 36: 791-794.